Thermal conductivity: a theoretically simple, yet practically challenging experiment

Thomas Gumpenberger[1], *Kanchan*[1] Dasgupta, and *Wolfgang* Hujer[1]

[1]OMV Exploration & Production GmbH, 1020 Wien, Austria

Abstract. We report on the first systematic investigation of thermal conductivities on a wide range of core samples from a variety of lithologies from the Vienna Basin, Austria. The investigated temperatures range from 15°C to 135°C. The first value is assumed for outcrops, the latter value is the highest temperature expected in regions of geothermal interest in the Vienna Basin. With the strategic shift towards de-carbonisation and renewed interest in geothermal projects, thermal conductivity measurements become an increasingly requested service for petrophysical laboratories. In a preliminary step, we investigated three experimental methods for thermal conductivity measurements with the help of external partners before settling on a steady state device directly employing Fourier's Law. Preliminary investigations for establishing a proper workflow revealed a "thermal history" of samples that we tentatively attribute to the effects of residual sample humidity. The effect exceeds deviations expected from different calibrations regimes and persists even after days of oven drying (60°C) and influences thermal conductivity recorded in a repeat experiment. It occurs when a temperature stage in a previous experiment exceeded the drying temperature. The absolute size of the effect correlates with overall thermal conductivity and lower sample porosity. Notable outliers are very fine-grained sandstones with higher porosity and comparably low permeability, where removal of residual humidity is slow and inefficient. Furthermore, great care is required during mechanical sample preparation, i.e., wedge errors need to be low and both end faces of the sample should exhibit as similar roughness/smoothness as possible. The latter property directly affects the thermal contact resistance, i.e., a temperature-drop at the device-sample interface. While thermal contact resistance can be eliminated by measuring two samples from the same core cut to different thicknesses, this approach fails for, e.g., conglomerates when the size of the components becomes large relative to the sample's dimension. The two individual samples are then too heterogenous to mathematically solve for "true" thermal conductivity. Additionally, we suspect that as residual humidity changes during the heating of the sample, contact resistance changes as well. Finally, sample preparation for friable sandstones remains technically challenging.

1. Introduction

Within the realm of special core analysis, thermal conductivity measurements have so far received scant attention. A keyword search for 'thermal' in the SCA archives from 1995 up to the time of compiling data for this paper provided only about ten papers, the majority of which investigated temperature effects as a source of experimental errors in SCAL [1]. Some researchers studied the influence of temperature as a parameter for thermo-poro-elastic (T-P-E) models [2, 3]. Others investigated the effects of the thermal history of rocks on permeability [4] or mechanical strength [5].

Thermal properties of rocks in their own right are discussed in [6] where the focus is "the effective thermal conductivity of an oil sand reservoir undergoing thermal production, adequate mixing rules that incorporate grain statistics, porosity, and relative contributions of the saturations and thermal conductivities of the constituent fluids and solids". The paper itself is short on experimental procedures and focuses more on the mathematical treatment of data but refers to the data acquisition options in [7].

Only from 2010 onward thermal properties start to appear as stand-alone topics. Reference [8] discusses the application of differential scanning calorimetry (DSC) on porous samples. However, the main product of DSC-measurements are heat-capacity c_P and the latent heats of phase transitions rather than thermal conductivity.

* Corresponding author: Thomas.gumpenberger@omv.com

Finally, Popov [9] presents a systematic investigation into the thermal properties (conductivity, diffusivity and heat capacity) of a wide range of rock and core samples based on an optical scanning technique.

A second search for "geothermal" produced some papers discussing the characterisation of geothermal plays/formation by classical core analysis [10, 11, 12] as well as various publications containing the search string within the authors' affiliations. In summary, few if any papers were found in the SCA-Archives discussing thermal conductivity either as a dedicated experimental procedure or as part of reservoir characterisation.

2. Motivation and evaluation of experimental techniques

2.1. Motivation

About three years back the authors' employer made a strategic shift towards low-carbon business and laboratory technologies had to be adapted to reflect this change in demand. Heat capacity as a laboratory product was ruled out, as the majority of rock-forming minerals cluster tightly around values of 800 J/kg*K [13]. Furthermore, these values are typically dwarfed by that of the heat capacity of water (4184 J/kg*K). In addition, heat capacity being a scalar property, heat in place can readily be calculated by arithmetic averages, taking into account rock porosity.

Thermal conductivity, on the other hand, covers a much wider range of values. Even for the same substance (pure SiO_2) the values differ markedly based on modification: 1.35 W/m*K and 7.68 W/m*K for fused and crystalline quartz, respectively. For pyrite values as high as 19.2 W/m*K are reported [all data from 14]. In natural rocks geometric factors and the saturation state can further alter macroscopic thermal conductivity. Heat can be transported both by a stagnant or moving fluid, conduction along grain contacts and even thermal radiation in the pore space [15].

2.2. Evaluation of available techniques

Prior to committing to the purchase of a dedicated device, samples of various lithologies were sent to external partners (universities and vendors) for the evaluation of different experimental methods. Samples were representatives for sandstone, conglomerate, granite, and carbonate taken from OMV's core storage. Representative samples were cut and distributed to partner laboratories. The test thus resembled a "round robin" test looking at consistency in the results across various techniques and operators, even though the true thermal conductivity values were unknown.

2.2.1. Needle probe

A TK04 device from TeKa, Germany was employed. The needle-probe simultaneously serves as a line source for heat as well as a temperature sensor. The mathematical model assumes ideal heat contact at the probe and energy decay into an infinite half space. Experimentally, surface effects at the central bore need to be discarded and data acquisition needs to stop once the effects of the finite sample's boundaries are felt.

The system's software automatically chooses the largest valid measurement interval based on the concept of "logarithm of extreme time" LET. A derivation of the mathematics can be found in reference [16 (German)].

2.2.2.HotDisk Sensor

This technology is a variation of the needle probe system. Here, rather than a line source an area source is used, typically incorporated into a polymer strip (Kapton or Teflon). For high temperature applications (up to 1000°C according to the vendor) mica-based sensors are available. The sensor is placed on either the end face or between two disks of the material under investigation.

2.2.3. Steady state techniques

Devices based on steady state simply employ Fourier's Law (1)

$$\boldsymbol{q = -k\nabla T} \tag{1}$$

where q is the heat flux [W/m²], k the thermal conductivity [W/m*K], and ∇T [K/m] the temperature gradient.

Briefly, a disk of sample material is sandwiched between two plates of the device which are then kept at different, constant temperatures. Heat flow meters (HFM) in both plates record the heat flux into (hotter plate) and out of (cooler plate) the sample. The HFMs consist of dozens of small thermocouples that are bonded to the surfaces of both plates and cover the central (~25 by 25 mm) section of the sensor. Preliminary investigations (data not presented) showed that the sample diameter should be at least 45 mm. This allows for a linear thermal gradient unaffected by edge effects to develop in the central portion of the sample.

In this one-dimensional application the term ∇T from (1) simplifies to $\frac{\Delta T}{\Delta x}$, where Δx denotes sample thickness.

The experiment can be run both in "1dx" and "2dx" mode. The heat transfer at the sample's surfaces is not ideal (e.g., due to roughness). This causes an additional temperature drop at the surface affecting the calculation of k when measuring the sample at only one thickness (1dx mode). By measuring at two different thicknesses (2dx mode) this effect can be mathematically removed – assuming the samples have the same composition and surface texture.

2.3. Result of evaluation

Aggregated results are shown in Tab. 1. Data are averages of three measurements and were recorded on dry samples at ambient temperature.

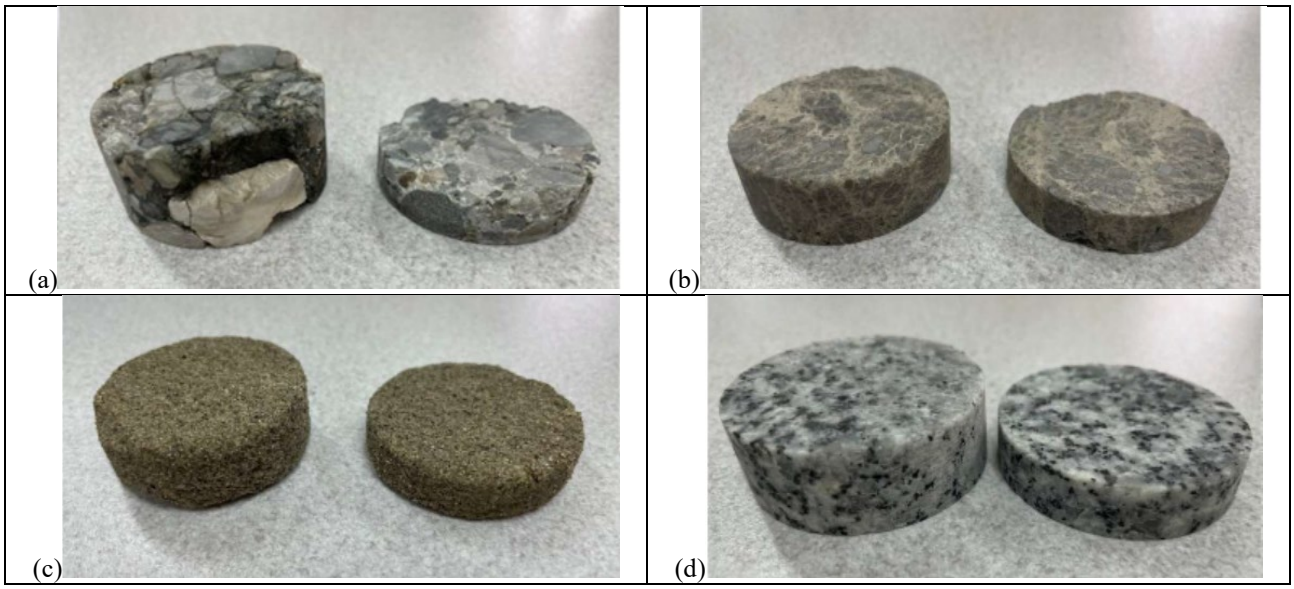

Fig. 1. Samples used for the evaluation: representatives for conglomerate (a), dolomite breccia (b), sandstone (c), and granite (d).

Tab. 1. Results of the evaluation. SS = sandstone, Congl. = conglomerate, Carb. = carbonate. All values in W/m*K.

	Steady state			Transient	
	Uni 1 2dx	Uni 1 1dx	Uni 2 1 dx	Needle	HotDisk
SS	4.21	0.61	0.44	0.16	0.92
Congl.	1.81	2.23	2.44	3.06	2.30
Granite	3.43	2.69	2.80	2.82	3.56
Carb.	3.62	2.79	3.59	3.59	4.52

Images of the sample used for this test are presented in Fig. 1. Results on sandstone exhibit a large difference between the 2dx steady state method and the rest. This indicates strong effects of surface roughness/coupling of heat. Polishing options for sandstones are limited by friability and grain size.

Conglomerate samples are more amenable to polishing where required but exhibit large heterogeneity as apparent in Fig. 1 to which we tentatively attribute the variation of the results.

Results for the granite sample show two groups (around 2.8 and 3.6 W/m*K, respectively) with no ready explanation available.

Finally, for the carbonate the "consensus" value appears to be 3.6 W/m*K with outliers above and below.

2.4. Conclusions from evaluation

The authors eventually decided on procuring a steady state device based mainly on the following considerations:

- Samples for the needle probe require a large sample volume (full core) that is not always available. Further, drilling long, narrow, smooth holes presents a technical challenge.
- Both needle probe and HotDisk record thermal conductivity at the respective ambient temperature. For obtaining conductivity values at reservoir temperature additional ovens would be needed. This again requires further system automation (for temperature ramps) and a larger footprint in the laboratory.
- The 2dx mode of operation allows for compensating for the effects of thermal contact resistance (at least in theory).

3. Geothermal rock data base

3.1. Project description

Additional measurements were conducted within a project with the scope to create a database of thermal conductivities of lithologies encountered in the Vienna Basin, Austria. Overall, forty-seven (47) samples were selected from OMV's core storage representing:

Sandstones (23)	Carbonates (14)
Heterolithics (6)	Marlstone (2)
Anhydrite (1)	Granite (1)

Samples from hydrocarbon bearing formations were cleaned in soxhlet configuration using an azeotrope of methanol and chloroform. Samples from non-hydrocarbon bearing formations were used as-is. Salinity of aquifers in the Vienna Basin is low (3%) and the risk from salt precipitates considered low. All samples were stored at least for several days in an oven at 60°C and ambient pressure to ensure consistent initial conditions.

Investigated temperatures range from 15°C up to 135°C. The first value is considered representative for outcrop conditions, the latter value is the highest temperature expected in regions of geothermal interest in the Vienna Basin. Due to time constraints, only 1dx measurements on thick samples (3.5 cm) were recorded initially, as here the effect of thermal contact resistance is relatively weaker (see Fig. 2). For reference, total instrument time for the data set was in the order of 800 hours.

The temperature difference between the two plates was 10°C for all experiments. Due to limitations in the device's software not all temperatures could be automatically recorded in one run (dubbed low- and high-

temperature run, respectively). Additionally, different calibration standards were needed for different temperature ranges. For the range between -10°C and 110°C Pyrex glass can be used a reference standard. Calibrations are stable over the duration of at least a year (Fig. 2).

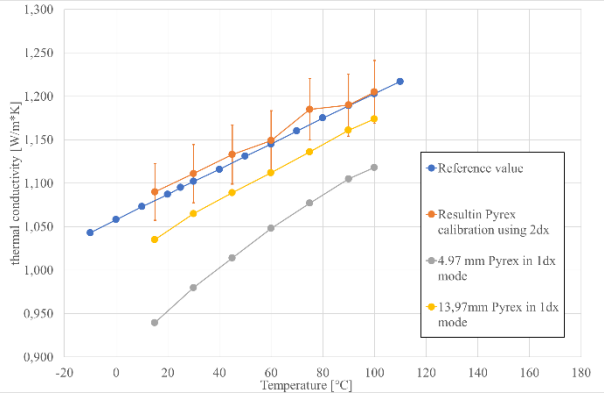

Fig. 2 tabulated conductivity values (blue), result of 2dx measurement of the calibration standard >1year after calibrating the device (orange), individual 1dx measurements in yellow and grey. Note that the thermal contact resistance affects thinner samples more.

We also checked the samples for wedge errors by recording sample thickness at 45° intervals around the circumference of the samples. The maximum observed standard deviation was ~120 µm. The obtained thicknesses show excellent agreement with data automatically obtained by the device (not shown).

Where possible, surface roughness values Ra were obtained by means of Mitutoyo SJ-210 Surface roughness measuring device. Briefly, a cantilever with a diamond stylus of 2 µm radius is scanned across the surface of interest and the deflecting force is recorded. The surface roughness is then calculated from the deflections after correcting for long range changes in surface morphology using Gaussian filters. All the mathematical processing is done by the device. As indicated above, not all samples could be investigated as, e.g., fractures across a sample's surface would exceed the cantilever's range of motion, causing the device to abort the measurement.

In total, measurements could be performed on 34 out of the set of 47 samples. The average roughness was 12.5 µm for sandstones, 8.1 µm for heterolithics, 3.5 µm for marlstones, and 2.5 µm for carbonates.

3.2. Results

Aggregate data for all measurements are presented in Fig. 3. Depending on the investigated temperature the recorded conductivity values range from 0.8 W/m*K to 4.8 W/m*K.

As a general observation, sandstones and hetherolitics exhibit a lower thermal conductivity than carbonates. Granite plots to the centre of the range, albeit only one representative is included in the data set. Similarly, marlstones on average exhibit a lower conductivity than sandstones, with two samples in the dataset. The highest value was recorded on the anhydrite sample.

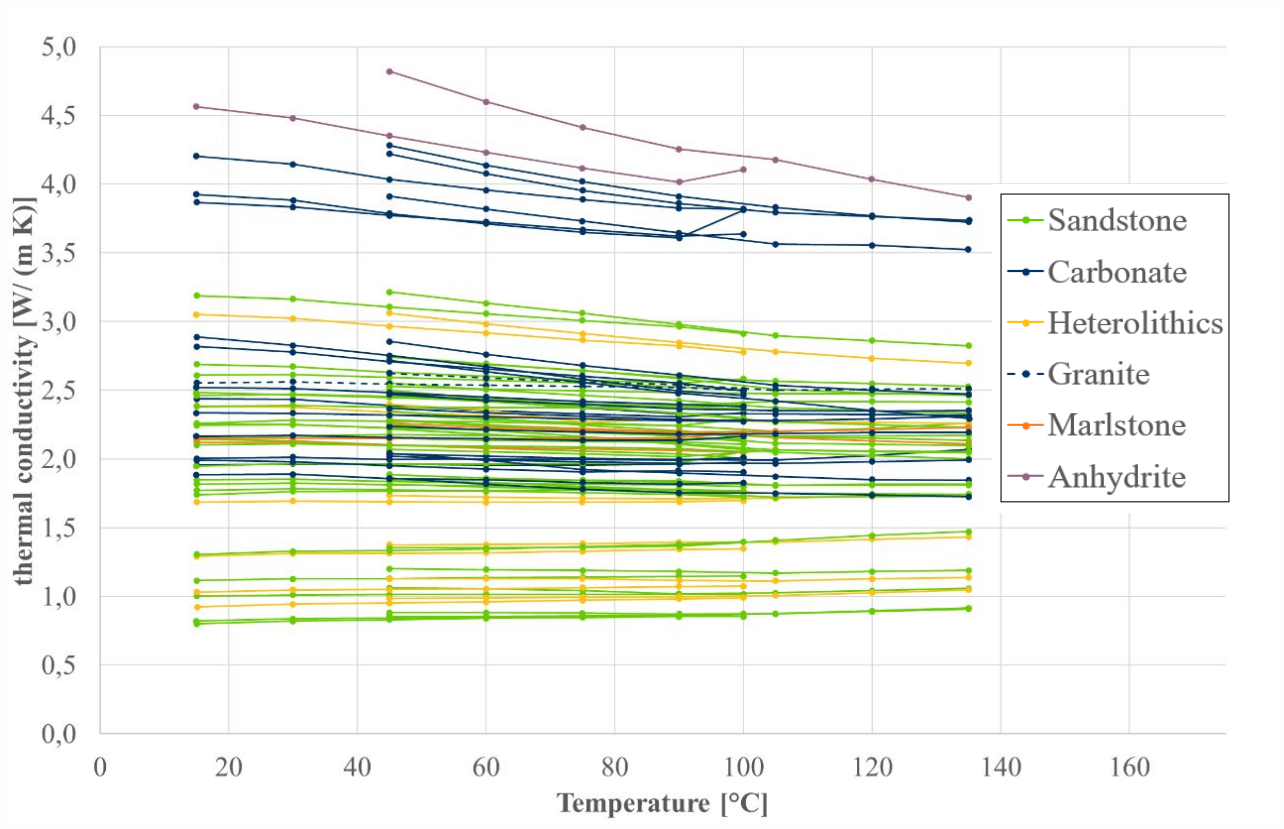

Fig. 3 aggregate view of thermal conductivities; green = sandstones, blue = carbonates, yellow = hetherolithic, dashed blue= granite, orange = marlstone, and purple = anhydrite

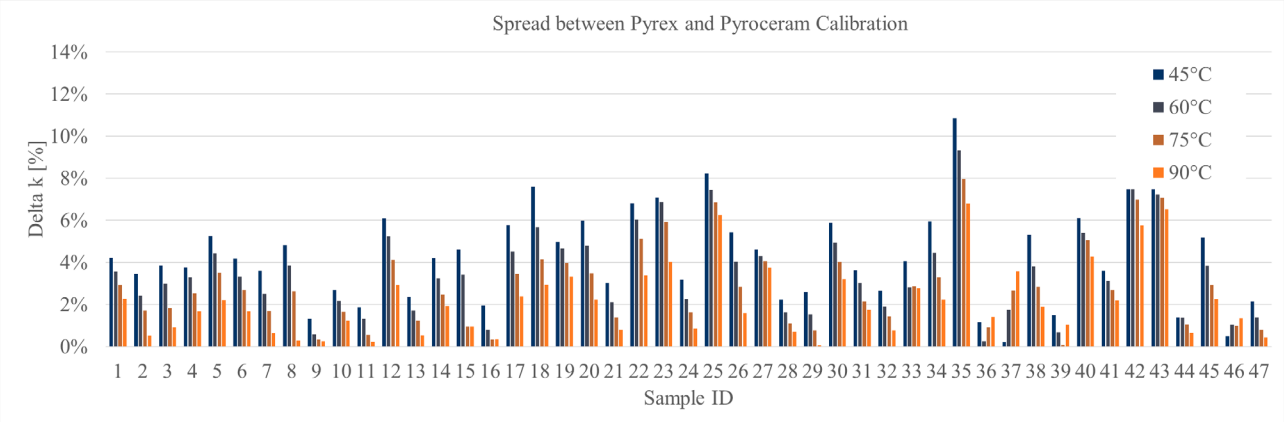

Fig. 4 difference between thermal conductivities obtained using Pyrex or Pyroceram as calibration standard at four temperatures. The difference is expressed in percent of the average thermal conductivity value at that temperature. The step like pattern can be motivated by a systematic error, the amount of the error appears to depend on additional factors.

Early into the measurement campaign it was noted that data obtained at the overlap of low and high temperature run exhibited a distinct "jump". Systematic investigation of the effect revealed the patterns in Fig. 4. The percentage deviation in many cases is larger than the 3% uncertainty specified by the vendor.

The general trend of the deviations at the four temperatures (45, 60, 75 and 90°C, respectively) covered by both low- and high temperature run can partially be explained by the use of a different calibration standard (Pyroceram) at higher temperature ranges. Recording data of a Pyrex calibration standard using a Pyroceram calibration in the device resulted in higher-than-expected conductivity values. The match with tabulated data improved with increasing temperature. This is reflected in the step pattern observed in nearly all samples.

However, indications for another phenomenon affecting the extent of the effect were:

- The effect got smaller upon repeating the experiment within the same calibration.
- The effect worsens with decreasing sample thickness.

3.3.Effects of repeated measurement

For selected samples, where a high mismatch was observed, the measurement was repeated. Typically, the data points would converge, and the spread be reduced (Fig. 5).

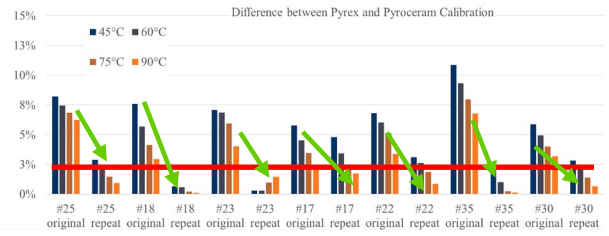

Fig. 5 same data as in Fig. 4 for repeat experiments for selected samples. The spread drops in repeat experiments (green arrows). The red line indicates the 3% precision specified by the vendor.

We tentatively attribute this effect to some remaining moisture in the sample. The effect appears to correlate negatively with sample porosity (not shown, the "worst offender" was the anhydrite sample). Presumably even prolonged vacuum drying at 60°C cannot fully remove humidity from the pore space. A working hypothesis – even though the exact mechanism is unclear at this stage – is that humidity affects the coupling of heat into the sample. This is indicated by the fact that thinner samples show a larger scatter in data as discussed below.

3.4. Thermal history and sample thickness

The effect of sample thickness on instrument performance is shown exemplarily on three of the "worst offenders" in Fig. 6 to Fig. 11. The first sample was a fine-grained sandstone of 7.5% porosity. The sample was initially measured at 35 mm thickness and then cut in to two slices of 12 and 20 mm. Since the cutting process involved cooling water, samples were now dried in 60°C in vacuum for two days, rather than storage at 60°C at atmospheric pressure.

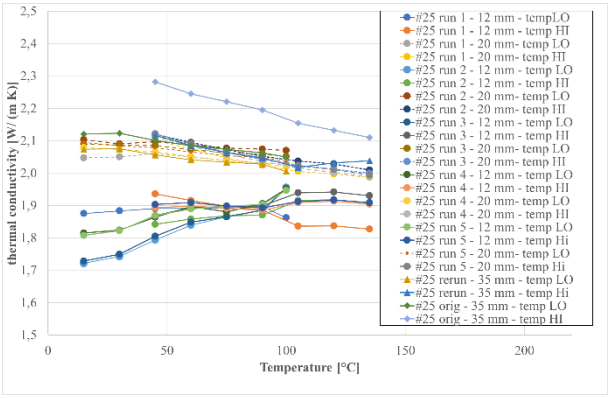

Fig. 6 thermal conductivity data obtained on one and the same sandstone sample (#25). 35 mm: full line diamonds and triangles, 20 mm: dashed lines, 12 mm: solid lines circles

Upon repeating the measurement, the outlier from the first measurement collapses into the upper cluster, where

data from 35 mm and 20 mm thick samples overlap. In general, a trend of decreasing conductivity with increasing temperature can be discerned for this cluster. In contrast, data obtained on the thinner (12 mm) slice show a remarkable scatter, particularly at lower temperatures, even when using the same calibration.

A possible explanation is the effect of ambient humidity between measurements. While the instrument can be operated via remote, it cannot be setup to repeat measurements independently. Thus, if the instrument finishes a run at night, the sample will be exposed to the atmosphere until the next morning. In a final step, to ensure proper removal of moisture, the first data point was set to a temperature of 120°C. Any latent heat from the expulsion of humidity would disturb the equilibration of the heat flow sensors. Only after equilibrium (= dry state) is achieved, data would be recorded. The results are presented in Fig. 7.

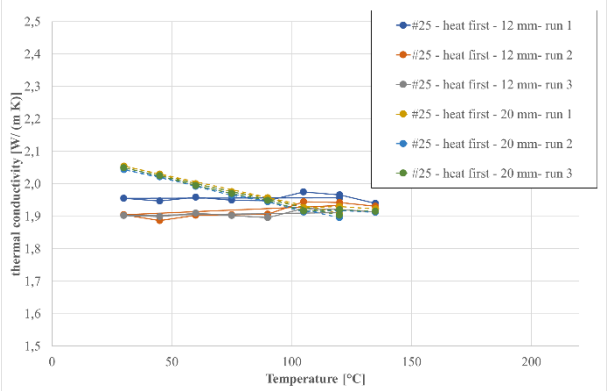

Fig. 7 same data as in Fig. 6, this time with the first data point recorded at 120°C 20 mm: dashed lines, 12 mm: full lines. The 35 mm sample was no longer available.

Note that the axes in Fig. 7 are scaled identically as in Fig. 6. Data from the 20 mm slice collapse into a single line. Scatter for the 12 mm slice is drastically reduced, even though here the first measurement records data slightly higher than runs 2 and 3.

This observation was confirmed by data from different rock types. Fig. 8 and Fig. 9 show the same data obtained on anhydrite.

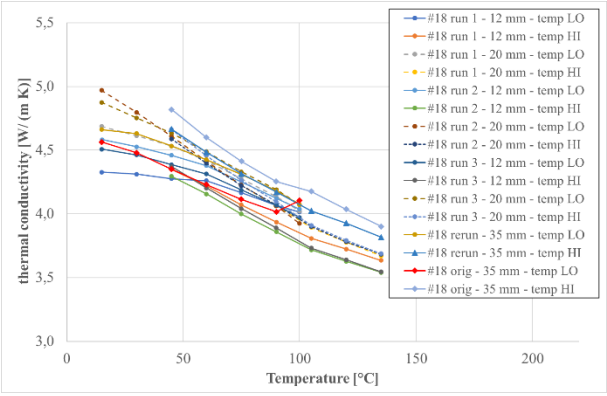

Fig. 8 thermal conductivity data obtained on anhydrite sample cut to different thicknesses. 35 mm: full line diamonds and triangles, 20 mm: dashed lines, 12 mm: solid lines circles. Note the jump when the sample is first heated above 100°C (red diamonds)

Again, when the temperature at the first data point exceeds 100°C, the scatter in repeated measurements is drastically reduced. Note again that axes in Fig. 8 and Fig. 9 are identically scaled.

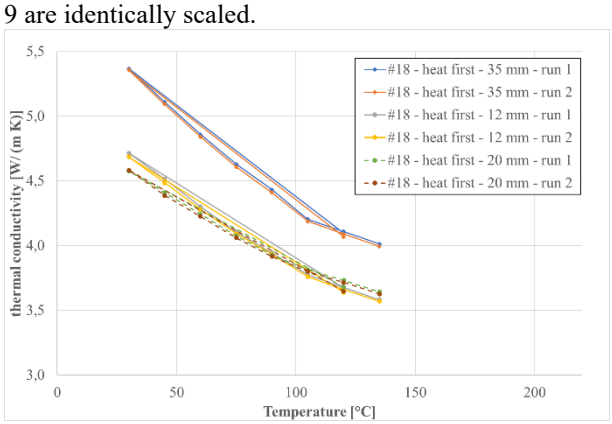

Fig. 9 same data as in Fig. 8, this time with the first data point recorded at 120°C 20 mm: dashed lines, 12 mm: full lines + circles, 35 mm: full lines + diamonds.

The same behaviour can also be seen on granite (Fig. 10 and Fig. 11, both graphs identically scaled).

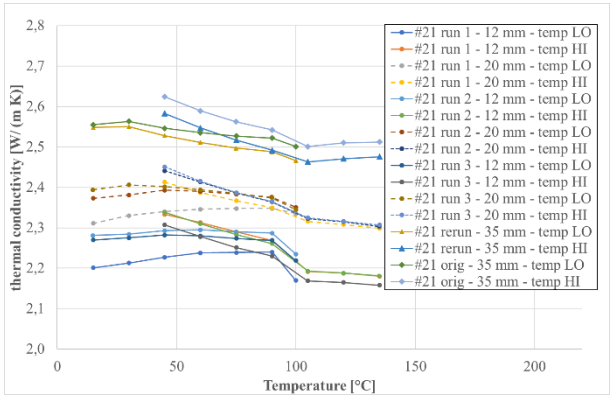

Fig. 10 thermal conductivity data obtained on granite. 35 mm: full line diamonds and triangles, 20 mm: dashed lines, 12 mm: solid lines circles

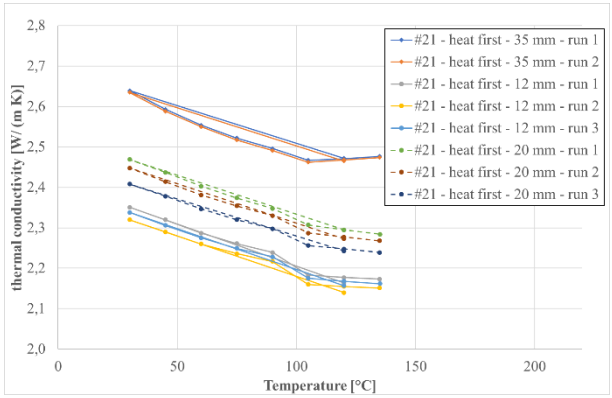

Fig. 11 same data as in Fig. 10, this time with the first data point recorded at 120°C 20 mm: dashed lines, 12 mm: full lines + circles, 35 mm: full lines + diamonds

3.5. Extreme case with water and Berea sandstone

As test of an extreme case, we deliberately wetted a piece of Berea sandstone (Fig. 12). As expected, recorded conductivities were higher than for dry rock. However, two anomalies are observed.

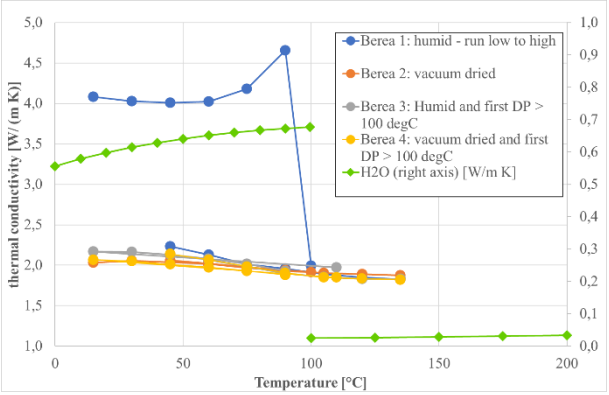

Fig. 12: thermal conductivity of deliberately wetted Berea. Note that reference values for water (diamonds) are plotted to the right ordinate scale.

Naively one expects conductivity of a wet rock to be bound by the limits of Lichtenecker's mixing rule for a rock saturated with a single fluid (gas, brine, oil)

$$\lambda^k = (1-\phi)\lambda_m^k + \phi\lambda_p^k \qquad (2)$$

Here, Phi is porosity, the indices m and p denote matrix and pore fluid, respectively, and k is from [-1;1]. As can easily be seen, the limiting cases result in the well-known formulas for serial and parallel configuration of conductivities.

Assuming a reasonably reliable bulk thermal conductivity at 75°C of ~2 W/m*K (at 20% porosity this implies a thermal conductivity of the matrix of ~2.5 W/m*K, in agreement with [14]), saturating the pore space with water (0.65 W/m*K) would only add 0.13 W/m*K to overall conductivity for a total of 2.13, not the recorded 4.18 W/m*K. However, similar values reported in [17, Fig. 6d]. A recent paper from Pichugin [18] suggests that traditional mixing rules underestimate thermal conductivity.

Secondly, while the thermal conductivity of water rises with temperature (from 0.57 to 0.67) in the investigated range, thermal conductivity rises by 0.6 W/m*K, before it drops to the value of dry rock at 100°C.

3.6. Applying 2dx corrections

Based on the effects described in sections 3.4 and 3.5, we attempted to correct for the temperature jump at the sample surface by applying the 2dx correction (exemplarily on a tight sandstone, Fig. 13) to data obtained on samples where the first data point was obtained above 100°C. Derived 2dx conductivity values increase markedly over the 1dx data. However, at higher temperatures, where results from the 12 mm and 20 mm samples are very close to each other, the algorithm produces unphysical results in the sense that the corrected values lie below the input data.

Another obvious complication were heterogeneous samples with clast whose sizes approached the order of the sample thickness (data not shown). Here, the underlying assumption of a homogeneous material at different thicknesses is simply not fulfilled.

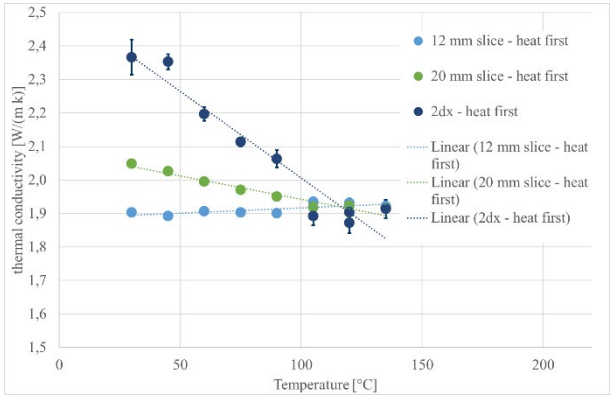

Fig. 13 applying the 2dx process (dark blue) to conductivity data obtained on sandstones of 12 mm (light blue) and 20 m (green). Error bars on 1dx measurements are smaller than the symbols.

4. Conclusions and recommendations

Where do we go from here and what conclusion to draw from this data if we want to properly determine thermal conductivities? We suggest at least to observe the following recommendations:

- The experiments are by their nature time consuming. If time is a constraint, use the thickest possible cut of sample possible and record data in 1dx mode.
- Avoid wedge errors in the samples and polish the surfaces. We obtained good results using 120 and 320 grit silicon carbide paper. Note that for sandstones the achievable surface roughness is limited by grain size and friability.
- Most importantly, from the perspective of the authors, create standardized initial conditions for all samples by removing any trapped humidity by choosing the first recording temperature above 100°C.

One might object to the last point that too high temperatures may alter the mineral structure by removing the water of crystallization (as e.g., in gypsum). In practice this should be without consequence. Projects that mostly rely on thermal conductivity as input parameter (hot and dry wells run with heat exchangers) are typically at higher temperatures in the first place.

In summary, despite a fundamentally simple experimental setup, obtaining thermal conductivity data on rocks has its pitfalls. As we performed the first systematic investigation of thermal conductivities on a wide range of core samples from a variety of lithologies from the Vienna Basin, Austria, the combined effects of surface roughness, sample heterogeneity and residual humidity lead to higher-than-expected scatter in repeat measurements than expected from device specifications.

References

1. D. R. Maloney, K. L. Doggett, SCA1995-030 (1995).
2. R. Ashena, G. Thonhauser, H. Ott, V. Rasouli, S. Azizmohammadi, M. Prohaska, SCA2017-026 (2017).
3. S. Govindarajan, M. Aldin, A. Thombare, O. Abdulbaki, D. Gokaraju, A. Mitra, R. Patterson, SCA2022-003 (2022).
4. Z. Bin, L. Li, and L. Qingjie, SCA2022-054 (2022).
5. T. Livada, A. Nermoen, R. I. Korsnes, I. L. Fabricius, SCA2016-087 (2016).
6. J. Arthur, E. Skripkin, S. Kryuchkov, A. Kantzas, SCA2016-092 (2016).
7. J. K. Arthur, O. Akinbobola, S. Kryuchkov, A. Kantzas, SPE174434-MS (2015).
8. E. Dyshlyuk, SCA2013-055 (2013).
9. Yu. Popov, D. Korobkov, D. Miklashevskiy, S. Safonov, S. Novikov, SCA2010-010 (2010).
10. H. Pape, C. Clauser, J. Iffland, J. Bartels, R. Wagner, M. Kühn, SCA2001-060.
11. W. Hübner, J. Orilski, M. Halisch, T. Wonik, SCA-2010-041 (2010).
12. A. Ali, K. Miah, D.K. Potter, SCA2012-049 (2012)
13. D. W. Waples, J. S. Waples, Natural Resources Research, **13 (2)** (2004).
14. K. Horai, G. Simmons, Earth and Planetary Science Letters **6**, 359-368 (1969).
15. D. Kunii, J. M. Smith, AIChE Journal **6 (1)**, p 71-77 (1960).
16. K. Erbas, Dissertation at the Technical University of Berlin (in German) (2012).
17. W. Lin, O. Tadai, T. Hirose, W. Tanikawa, M. Takahashi, H. Mukoyoshi¸ M. Kinoshita, Geochem. Geophys. Geosyst **12 (6)** (2011).
18. Z. Pichugin, E. Savelev, E. Chekhonin, Y. Popov, M. Kalinina, I. Bayuk, E. Popov, M. Spasennykh, R. Romushkevich, S. Rudakovskaya, Geothermics **104 (3)**, p 102456 (2022).